Docosahexaenoic acid attenuates Western diet-induced hepatic fibrosis in *Ldlr*$^{-/-}$ mice by targeting the TGFβ-Smad3 pathway[S]

Kelli A. Lytle, Christopher M. Depner, Carmen P. Wong, and Donald B. Jump[1]

Nutrition Program, School of Biological and Population Health Sciences, Linus Pauling Institute, Oregon State University, Corvallis, OR 97331

Abstract **DHA (22:6,ω3), but not EPA (20:5,ω3), attenuates Western diet (WD)-induced hepatic fibrosis in a *Ldlr*$^{-/-}$ mouse model of nonalcoholic steatohepatitis. We examined the molecular basis for the differential effect of dietary EPA and DHA on WD-induced hepatic fibrosis. DHA was more effective than EPA at preventing WD-induced effects on hepatic transcripts linked to fibrosis, including collagen 1A1 (Col1A1), transforming growth factor-β (TGFβ) signaling and proteins involved in remodeling the extracellular matrix, including metalloproteases, tissue inhibitors of metalloproteases, and lysyl oxidase subtypes. Examination of the TGFβ pathway showed that mice fed the WD supplemented with either olive oil or EPA had a significant (⩾2.5-fold) increase in hepatic nuclear abundance of phospho-mothers against decapentaplegic homolog (Smad)3 when compared with mice fed the reference diet (RD); Smad3 is a key regulator of Col1A1 expression in stellate cells. In contrast, mice fed the WD supplemented with DHA had no increase in phospho-Smad3 when compared with mice fed the RD. Changes in hepatic phospho-Smad3 nuclear content correlated with proCol1A1 mRNA and protein abundance. Pretreatment of human LX2 stellate cells with DHA, but not other unsaturated fatty acids, blocked TGFβ1-mediated induction of Col1A1. In conclusion, DHA attenuates WD-induced fibrosis by targeting the TGFβ-Smad3-Col1A1 pathway in stellate cells.**—Lytle, K. A., C. M. Depner, C. P. Wong, and D. B. Jump. **Docosahexaenoic acid attenuates Western diet-induced hepatic fibrosis in Ldlr$^{-/-}$ mice by targeting the TGFβ-Smad3 pathway. *J. Lipid Res.* 2015.** 56: **1936–1946.**

Supplementary key words nonalcoholic steatohepatitis • collagen1A1 • stellate cells • inflammation

Nonalcoholic fatty liver disease (NAFLD) is a significant public health burden in Western societies. NAFLD is defined as excess accumulation of liver fat (hepatosteatosis), mainly as neutral lipids consisting of triacylglycerols, cholesterol esters, and diacylglycerols. NAFLD ranges in severity from benign hepatosteatosis to nonalcoholic steatohepatitis (NASH) (1). NASH is defined as hepatosteatosis with inflammation and hepatic injury (2). Although simple hepatosteatosis is considered clinically benign, NASH is the progressive form of the disease that can lead to significant changes in hepatic morphology (hepatocyte ballooning) and injury (cell death and fibrosis).

The incidence of NAFLD has increased in parallel with the obesity epidemic in Western societies. In the general population, the prevalence of NAFLD is estimated to range from 6 to 33% (3), and ∼30–40% of individuals with hepatic steatosis progress to NASH (4). The prevalence of NASH ranges from 3 to 5% in the general population (3). NAFLD and NASH have high prevalence (⩾60%) in patients with type 2 diabetes (5). Additionally, NASH patients have higher mortality rates than NAFLD patients (6–8), and over a 10 year period, cirrhosis and liver-related death occurs in 20 and 12% of NASH patients, respectively (9). Because NASH can progress to cirrhosis, hepatocellular cancer, and liver failure (4, 10–14), it is the third most common cause for liver transplantation. NASH is projected to be the leading cause of liver transplantation in the United States by 2020 (15).

Hepatic fibrosis involves the increased production of extracellular matrix (ECM) from activated hepatic stellate cells and myofibroblasts infiltrating the liver. The liver has an underlayment of connective tissue composed of several

This work was supported by USDA, National Institute of Food and Agriculture grant 2009-65200-05846 and by National Institutes of Health grants DK 43220 and DK 094600.

Manuscript received 11 June 2015 and in revised form 27 August 2015.

Published, JLR Papers in Press, August 27, 2015
DOI 10.1194/jlr.M061275

Abbreviations: Col1A1, collagen 1A1; DAG, diacylglycerol; ECM, extracellular matrix; Elovl, fatty acid elongase; IL1β, interleukin-1β; Lox, lysyl oxidase; LoxL, lysyl oxidase-like; NAFLD, nonalcoholic fatty liver disease; NASH, nonalcoholic steatohepatitis; NFκB, nuclear factor κB; qRT-PCR, quantitative RT-PCR; RD, reference diet; Smad, mothers against decapentaplegic homolog; TIMP, tissue inhibitor of metalloprotease; TGFβ, transforming growth factor-β; TLR, toll-like receptor; WD, Western diet.

[1]To whom correspondence should be addressed.
e-mail: Donald.Jump@oregonstate.edu

[S] The online version of this article (available at http://www.jlr.org) contains a supplement.

collagen subtypes (16). Fibrosis resulting from hepatic damage is linked to increased extracellular deposition of type 1 collagen [collagen1A1 (Col1A1)], smooth muscle actin, elastin, fibronectin, and other proteins. Fibrosis is also associated with increased production of proteins from stellate cells and macrophages that are involved in ECM remodeling; these proteins include lysyl oxidase and lysyl oxidase-like subtypes involved in collagen cross-linking, metalloprotease subtypes (MMPs), and tissue inhibitors of metalloproteases (TIMPs). The relative abundance of these proteins affects fibrosis progression and severity.

We previously reported that *Ldlr*$^{-/-}$ mice fed a Western diet (WD) develop a NASH phenotype that recapitulates human NASH in obese patients, including obesity, hyperlipidemia, hyperglycemia, hepatic damage, hepatosteatosis, induction of multiple markers of inflammation, oxidative stress, and fibrosis (17, 18). The WD is moderately high in saturated fat and trans-fat (43% total calories), and simple sugar (30% total calories), and cholesterol (1.5 g%) and reflects a modern, but unhealthy, diet (19). Dietary (fat, cholesterol, and fructose), metabolic (hepatic or plasma NEFA, hepatic ceramide), endocrine (insulin and leptin), gut (endotoxemia and the microbiome), and genetic (patatin-like phospholipase domain containing three polymorphisms) factors have been implicated in the progression of benign hepatosteatosis to NASH (20–27).

We also reported that adding EPA (20:5,ω3) or DHA (22:6,ω3) to the WD affected diet-induced hepatic fibrosis. DHA was more effective than EPA at attenuating WD-induced hepatic fibrosis (17, 18, 28). Although EPA and DHA attenuated WD-induced dyslipidemia, neither EPA nor DHA affected WD-induced body weight, the percent of body fat, blood glucose, or plasma endotoxin. The effect of $C_{20\text{-}22}$ ω3 PUFA on hepatic fibrosis was established by histology and quantifying the expression of fibrosis markers (i.e., Col1A1 and TIMP1) (17, 18). DHA and EPA are known to attenuate inflammation, decrease fatty acid synthesis, and increase fatty acid oxidation (29). The finding that DHA attenuated WD-induced hepatic fibrosis in obese mice was unexpected.

Several clinical trials have reported that dietary ω3 PUFA supplementation lowered hepatic fat in obese children and adults with NAFLD (30–37), whereas other investigators report that dietary supplementation with fish oil (36) or EPA-ethyl esters (37) does not attenuate the histological features of the disease, like fibrosis. As such, human studies using ω3 PUFA to treat NAFLD/NASH have yielded mixed results. Our studies have established a difference in how specific ω3 PUFAs affect clinical features associated with NASH. Herein, we examined potential mechanisms to explain how DHA and EPA differentially affect WD-induced hepatic fibrosis. Our findings establish that dietary DHA interferes with the TGFβ-mothers against decapentaplegic homolog (Smad)3 signaling pathway in vivo and attenuates TGFβ-mediated induction of Col1A1 expression in human stellate cells. The outcome of these studies has the potential to influence the design of clinical studies in children and adults with NAFLD/NASH.

MATERIALS AND METHODS

Animals and diets

All procedures for the use and care of animals for laboratory research were approved by the Institutional Animal Care and Use Committee at Oregon State University. Male *Ldlr*$^{-/-}$ mice (C57BL/6J background, Jackson Laboratories) at 2 months of age were fed one of the following four diets ad libitum for 16 weeks; each group consisted of 8 male mice (17). The reference diet (RD) (Purina chow 5053) consisted of 13.5% energy as fat, 58.0% energy as carbohydrates, and 28.5% energy as protein. The WD (D12079B; Research Diets) consisted of 17% energy as protein, 43% energy as carbohydrate, and 41% energy as fat; cholesterol was at 1.5 g%. The WD was supplemented with olive oil (WD + O), EPA (WD + E), or DHA (WD + D). WD supplementation with olive oil, EPA, or DHA increased total fat energy to 44.7% and reduced protein and carbohydrate energy to 15.8% and 39.5%, respectively. Olive oil was added to the WD to ensure a uniform level of energy from fat, protein, and carbohydrate in all WD diets. Preliminary studies established that the addition of olive oil to the WD had no effect on development or progression of diet-induced NAFLD in *Ldlr*$^{-/-}$ mice. The $C_{20\text{-}22}$ ω3 PUFA in the WD + E or WD + D diets were at 2% total energy. This dose of $C_{20\text{-}22}$ ω3 PUFA is comparable to the dose consumed by patients taking Lovaza™ (GlaxoSmithKline) for treating dyslipidemia (38), and this dose increases plasma $C_{20\text{-}22}$ ω3 PUFA in mice to levels seen in humans consuming 4–6 g/d of $C_{20\text{-}22}$ ω3 PUFA (39–41). A description of the diets and diet effects on mouse plasma and liver lipid composition was previously reported (17). At the end of the 16 week feeding period, all mice were fasted overnight (18:00 to 08:00 the next day) and euthanized at 08:00 for the collection of blood and liver (17, 28).

Measurement of plasma adipokines and proinflammatory cytokines

Plasma adipokines (leptin and adiponectin) were quantified by ELISA (R and D Systems). Plasma proinflammatory cytokines were quantified using a cytometric bead array mouse inflammation kit (BD Biosciences, San Jose, CA). Quantitative measurements of IL-12, TNFα, IFNγ, MCP-1, IL10, and IL6 were determined by flow cytometry per the manufacturer's protocol. Data were acquired using FACSCalibur (BD Biosciences), and data analyses were done using FCAP Array Software version 3.0 (BD Biosciences). Plasma for these assays was obtained from mice described previously (17, 18).

Analysis of plasma Toll-like receptor-2 and -4 activators

Plasma levels of Toll-like receptor (TLR)-2 and TLR-4 activators used Hek-Blue™ mTLR2 and Hek-blue™ mTLR4 cells (Invivogen), respectively. Cells were grown in 96 well cell culture plates overnight in 200 μl of Hek-Blue Detection medium™ (Invivogen) and 10 μl of plasma from the previous study (17). The formation of a blue color, reflecting activation of the TLR-NFκB pathway, was quantified by absorbance at 620 nm. Standard curves with authentic TLR2 (PAM3SK4) and TLR4 (LPS-B5) agonists are shown in supplementary Fig. 1.

RNA extraction and quantitative RT-PCR

Total RNA was extracted from liver, and specific transcripts were quantified by quantitative RT-PCR (qRT-PCR) (17, 42). Primers for each transcript are listed in supplementary Table 1. Cyclophilin was used as the internal control for all liver transcripts, and hydroxymethyl bilane synthase was used as the internal control of RNAs isolated from LX2 cells in culture. Transcripts were also quantified by qRT-PCR using the mouse fibrosis array (PAMM-120ZE; SABioscience-Qiagen). Hsp90ab1 was used as

the internal control for array analysis. Transcripts and their acronyms are provided in supplementary Table 2. Results from these studies were analyzed online using RT^2 Profiler PCR Array Data Analysis version 3.5 (SABioscience).

Immunoblot analysis

The quantitation of hepatic proteins by immunoblotting was previously described (17). The antibodies used to detect Smad2/3, Smad4, phospho-Smad2/3, and GAPDH were obtained from Cell Signaling Technologies. The antibody for procollagen 1A was obtained from Santa Cruz Biotechnologies.

Hydroxyproline

Hepatic hydroxyproline was quantified using the Hydroxyproline Kit (Sigma, MAK008). The colorimetric assay was carried out according to the manufacturer's instructions.

LX2 cells

LX2 cells were obtained from SL Friedman (Mount Sani Medical School) (43, 44). LX2 cells are activated human hepatic stellate cells; they are maintained in DMEM with 5% FCS containing penicillin, streptomycin, and normocin. Cells were plated on 100 mm plastic petri dishes at ~100,000 cells/plate and grown to confluence. Cells were treated with fatty acids (at 25 μM) in endotoxin-free BSA (at 10 μM) during the growth phase. Fatty acids [oleic acid (18:1,ω9), arachidonic acid (20:4,ω6), and DHA (22:6,ω3)] were obtained from Nu-Chek Prep. Cells were treated with 100 pM recombinant-human TGF-β1 (R and D Systems) in media containing no fatty acids or BSA for 24 h. RNA was extracted for qRT-PCR as previously described (18). Human PCR primers are listed in supplementary Table 1.

For fatty acid analysis, confluent cells were washed twice with cold PBS. Cells were extracted for fatty acids and quantified by gas chromatography analysis (17, 45) or applied to a reverse-phase HPLC system for the quantitation of ^{14}C-labeled fatty acids as described (46).

Statistical analysis

Statistical analysis of data used one-way ANOVA and Tukey-HSD to detect significant differences between groups. Data were analyzed for homogenous variances by the Levine test. If unequal variances were detected, data were log-transformed. ANOVA analysis was performed on both transformed and untransformed data. The hydroxyproline data were analyzed by Student's *t*-test. Values are reported as mean ± SD. A P value ≤ 0.05 was considered significantly different.

RESULTS

Effect of the WD and ω3 PUFA on plasma factors linked to hepatic inflammation and fibrosis

Toll-like receptors (TLR2 and TLR4) have been linked to hepatic inflammation and fibrosis (47–50). We previously reported that feeding *Ldlr*$^{-/-}$ mice the WD increased plasma endotoxin (18), a gut-derived microbial factor that activates the TLR4 pathway (51). WD-induced endotoxinemia was associated with increased hepatic nuclear content of NFκB as well as multiple NFκB-regulated transcripts linked to hepatic inflammation (17, 18). EPA or DHA supplementation of the WD did not attenuate WD-induced plasma endotoxin (18). Herein, we use a cell-based approach to quantify plasma levels of bioactive TLR2 and TLR4 agonist. Feeding *Ldlr*$^{-/-}$ mice the WD + O diet increased TLR2 and TLR4 agonist activity by ~60% (**Fig. 1**). Although the WD + D diet significantly lowered TLR2 agonists in plasma, WD + E and WD + D failed to lower plasma TLR4 agonists. Failure of the ω3 PUFA-containing diets to suppress TLR4 agonist is consistent with our previous finding, which showed that dietary ω3 PUFAs do not attenuate WD-induced endotoxinemia (18).

Hepatic fibrosis is also linked to products derived from adipose tissue and cells involved in innate immunity, including adipokines and cytokines, respectively (52, 53). We quantified plasma leptin, adiponectin, IFNγ, interleukins (IL6, IL10, and IL12), monocyte chemoattractant protein-1 (MCP1), and TNFα. Of these, WD + O feeding significantly increased plasma leptin and TNFα (Fig. 1). Addition of EPA or DHA to the WD had no significant effect on plasma levels of TNFα or leptin. The effect on leptin was anticipated because plasma leptin levels parallel adiposity. WD-fed mice are obese, and including EPA or DHA in the WD had no effect on adiposity (17).

Effects of WD and ω3 PUFA on the expression of genes involved in fibrosis

Feeding *Ldlr*$^{-/-}$ mice the WD elevated hepatic expression of Col1A1, TGFβ1, and Timp1, and dietary $C_{20\text{-}22}$ ω3 PUFA attenuated this effect (17). Herein, we used the SABioscience qRT-PCR fibrosis array to get a broad assessment of the impact of diet on hepatic fibrosis. The heat map (**Fig. 2**) illustrates the results with samples from livers of mice fed the RD, WD + O, WD + E, or WD + D (8 mice/group). The pie charts represent quantitation of transcripts that changed significantly. When compared with the RD group, 38, 28, and 12 transcripts were significantly induced by the WD + O, WD + E, and WD + D diets, respectively. Only two transcripts [metalloprotease-3 (Mmp3) and caveolin1] were significantly suppressed by the WD +

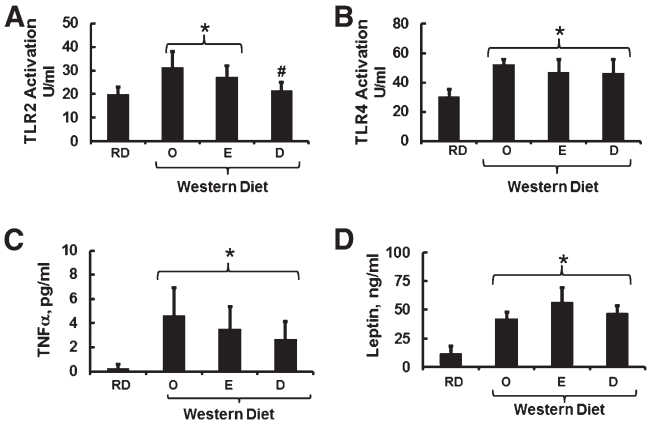

Fig. 1. Inflammatory and endocrine factors affecting liver fibrosis. Plasma levels of TLR2 (A) and TLR4 (B) activators were quantified using a cell-based assay as described in Materials and Methods. Results are represented as TLR activation units (U)/ml (n = 8; mean ± SD). The feeding groups were RD, WD + O, WD + E, and WD + D. Plasma TNFα (C) and leptin (D) were quantified as described in Materials and Methods. Results are expressed as pg/ml and ng/ml, respectively (mean ± SD; n = 8). *$P \leq 0.05$ versus RD; $^{\#}P \leq 0.05$ versus WD + O (ANOVA).

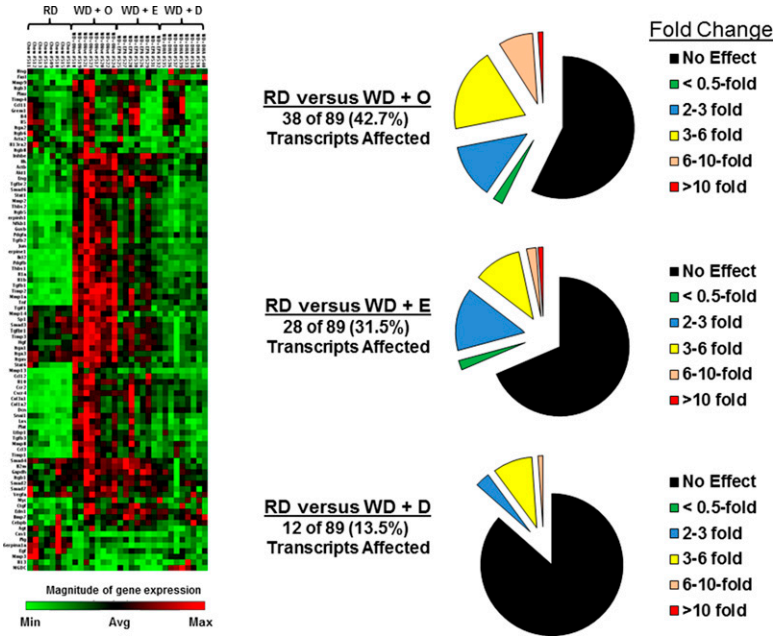

Fig. 2. Diet effects on the expression of genes involved in fibrosis. The mouse fibrosis array was used to quantify expression of 84 transcripts linked to fibrosis. The method uses a qRT-PCR approach. The heat map was generated using Qiagen online software and represents the relative abundance of transcripts. Each group had eight mice per group, and the groups were RD, WD + O, WD + E, and WD + D. The magnitude of gene expression was represented by green and red bars, indicating decreased and increased expression, respectively. The pie plots represent the number of transcripts affected by diet and the relative change in transcript abundance (fold change). Detailed analysis of transcripts is provided in Figs. 3–6 and supplementary Fig. 3.

O diet when compared with RD-fed mice. As illustrated in the heat map and in detailed quantitation of transcripts described below, the WD + D diet was more effective than the WD + E diet at attenuating WD effects on the expression of genes linked to fibrosis.

Collagen subtypes

Although the liver expresses several collagen subtypes (**Fig. 3**), Col1A1 is the major collagen subtype associated with hepatic fibrosis in WD-fed mice (17) and humans with NASH (16, 52). In normal mouse liver, Col1A1 and Col7A1 are expressed at low levels when compared with Col1A2 or Col4A. Using the qRT-PCR fibrosis array data (Fig. 2) as well as independent qRT-PCR analysis, WD feeding induced the expression of Col1A1, Col1A2, and Col4A1 by 17-, 5-, and 3-fold, respectively. Of these transcripts, only Col1A1 expression was significantly attenuated by dietary DHA. Dietary EPA did not attenuate WD-mediated induction of any collagen subtype.

ECM remodeling proteins

Fibrosis is associated with the induction of multiple proteins involved in remodeling the ECM, including metalloproteases, protease inhibitors, and enzymes involved in collagen cross-linking (**Fig. 4**). The mRNA abundance of three metalloproteases (Mmp1a, Mmp2, and Mmp13), four protease inhibitors (Timp1, Timp2, Serpine1, and Serpinh1), and the cross-linking enzyme lysyl oxidase (Lox) was significantly induced by WD + O. Although both WD + E and WD + E significantly attenuated the WD + O effect on the hepatic abundance of these transcripts, the WD + D diet was more effective than WD + E at attenuating expression of Mmp1a, Mmp2, Timp2, Serpinh1, and Lox.

Collagen crosslinking

Lox mRNA was induced by WD + O feeding and attenuated by WD + D > WD + E (**Figs.** 4 and **5**). Lox is one of several enzymes involved in collagen crosslinking. Lox and the lysyl oxidase-like (LoxL) family of enzymes are expressed in stellate cells and portal fibroblast (54). Accordingly, we quantified the effects of diet on the expression of Lox and LoxL subtypes (LoxL1, LoxL2, and LoxL3). In RD-fed mice, hepatic LoxL1 and LoxL3 are more abundant than Lox and LoxL2. Lox and all LoxL subtypes were induced (≥4-fold) by WD + O feeding. Feeding mice the WD + D diet attenuated the expression of Lox, LoxL1, and Loxl2 but not LoxL3. Expression levels of Lox and all LoxL subtypes in WD + O- and WD + E-fed mice were not different.

We also quantified hepatic levels of the product of Lox and LoxL1-3 activity (i.e., hydroxyproline) (Fig. 5C). Hydroxyproline levels were highly variable in livers from WD + O-fed mice. Hydroxyproline increased in three of the eight mice to levels >6-fold above the mean value quantified in RD-fed mice and mice fed WD + E or WD + D. WD + E and WD + D attenuated hepatic hydroxyproline content when compared with mice fed WD + O.

TGF-β Superfamily

TGF-β plays a major role in promoting fibrosis (48). Accordingly, we examined the TGFβ superfamily for diet

JOURNAL OF LIPID RESEARCH ASBMB JLR

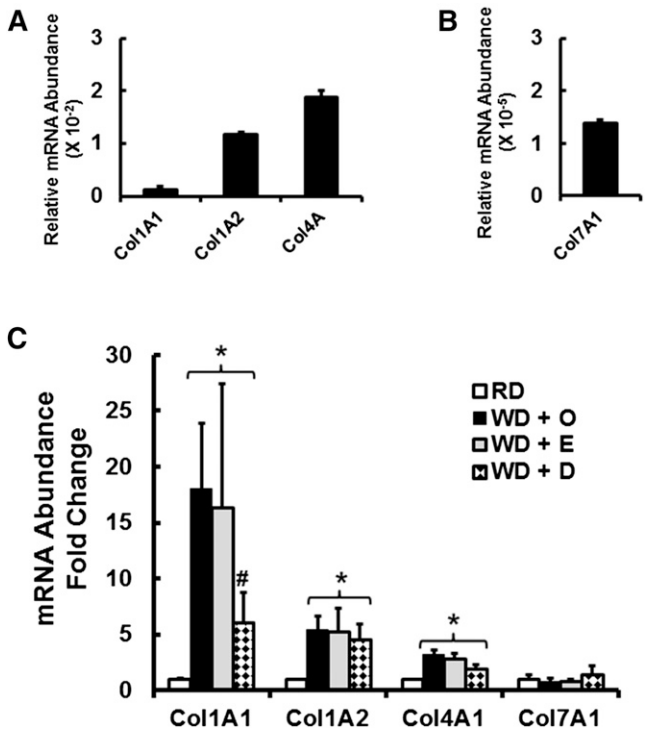

Fig. 3. Diet effects on hepatic collagen subtype expression. Expression of hepatic collagen subtypes used qRT-PCR and primers listed in supplementary Table 1. The upper panels represent relative mRNA abundance of the collagen subtypes in mice maintained on the RD; cyclophilin was the reference transcript. The lower panel represents the fold change in hepatic expression of the collagen subtypes of mice fed the RD or the WD + O, WD + E, or WD + D diets. Results are expressed as fold change (mean ± SD; n = 8). $^{*}P \leq 0.05$ versus RD; $^{\#}P \leq 0.05$ versus WD + O.

effects on gene expression (**Fig. 6**). Mice fed the RD express three TGFβ subtypes in liver; the relative abundance of the three transcripts is: TGFβ1, 1.0 ± 0.1; TGFβ2, 0.031 ± 0.01; TGFβ3, 0.06 ± 0.013. Of these, TGFβ1 is the predominant hepatic TGFβ subtype. Feeding mice the WD + O diet induced all three TGFβ subtypes (2- to 3-fold). The

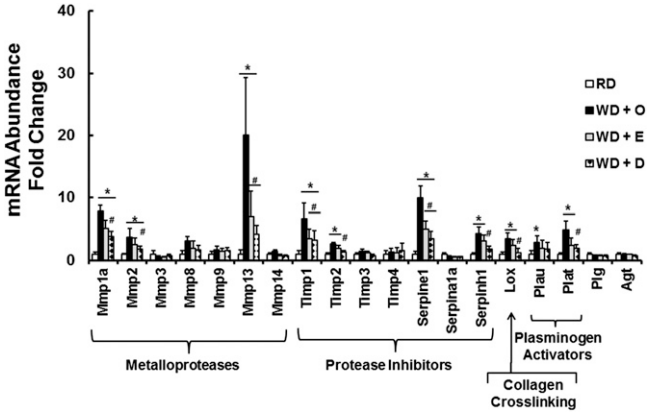

Fig. 4. Diet effects on expression of remodeling enzymes. Transcript abundance of proteins involved in extracellular matrix remodeling was quantified using data from the qRT-PCR array described in Fig. 2. Results are represented as mRNA abundance-fold change (mean ± SD; n = 8). $^{*}P \leq 0.05$ versus RD; $^{\#}P \leq 0.05$ versus WD + O.

WD + O diet also increased expression of the TGFβ receptor subunit-2 (Tfgbr2, 2-fold), Smad 6 (Smads are transcription factors and downstream targets of TGFβ signaling) (~2-fold), and two proteins that regulate TGFβ function [thrombospondins (Thbs1, Thbs2), 3- to 5-fold]. No significant difference was detected in the expression of these transcripts in mice fed the WD + O and the WD + E diets. Feeding mice the WD + D diet, however, significantly attenuated expression of all TGFβ subtypes, both TGFβ receptor subunits, Smad6, Thbs1, and Thbs2 when compared with WD + O-fed mice. As such, DHA, but not EPA, attenuates multiple transcripts associated with TGFβ signaling.

TGFβ Signaling

To further explore the impact of the WD and ω3 PUFA on TGFβ signaling, we examined the pathway for TGFβ induction of Col1A1 expression. TGFβ binds to type 1 and type II TGFβ receptors; TGFβ binding promotes recruitment of Smad2 and Smad3 to the TGFβ receptor complex where Smad2 and Smad3 are phosphorylated (55–60) (**Fig. 7A**). Smad2 is phosphorylated at S^{465} and S^{467}, whereas Smad3 is phosphorylated at S^{423} and S^{425}. Phospho-Smads move from the cytosol to the nucleus in association with Smad4. Binding of phospho-Smad3 to the Col1A1 promoter is associated with increased Col1A1 gene transcription and the accumulation of Col1A1 mRNA and protein (59).

Total and phosphorylated Smad2 and Smad3 were quantified in cytosol and nuclear extracts from livers of mice fed the RD or the WD + O, WD + E, or WD + D diets. Total hepatic Smad2 and Smad3 levels remained unchanged by diet. Although the antibody for phospho-Smads recognized both phospho-Smad 2 and phospho-Smad3, the position of the phosphorylated protein in the immunoblot corresponded to phospho-Smad3. Feeding mice the WD + O and WD + E diets significantly increased cytosolic and nuclear phospho-Smad3, reflecting activation of the TGF-β pathway. Feeding mice the WD + D diet, however, showed no increase in cytosolic or nuclear phospho-Smad3. Changes in nuclear phospho-Smad3 paralleled changes in Col1A mRNA (Fig. 3C) and proCol1A protein abundance (Fig. 7B and D). Although the WD + O and WD + E diets activate the TGFβ-Smad3 pathway and promote fibrosis, feeding mice the WD + D diet attenuates this pathway.

DHA attenuates TGFβ induction of Col1A1 in LX2 cells

The induction of Col1A1 expression in stellate cells is in response to increased production of TGFβ and cytokines (e.g., IL-1β) from hepatocytes, Kupffer cells, macrophages, and T-cells (53, 56–59). Herein, we determine whether DHA can act directly on stellate cells to regulate TGFβ1 control of Col1A1. LX2 cells are a human activated stellate cell line (43, 44). We first determined if LX2 cells assimilate and metabolize exogenous fatty acids. Accordingly, LX2 cells were treated with 25 μM fatty acids for 96 h to enrich cellular lipids (**Fig. 8A**). Treatment of cells with fatty acids (at 25 μM) had no adverse effects on cell growth or morphology. Fatty acid analysis shows that treatment of cells with fatty acids increased the cellular content of fatty

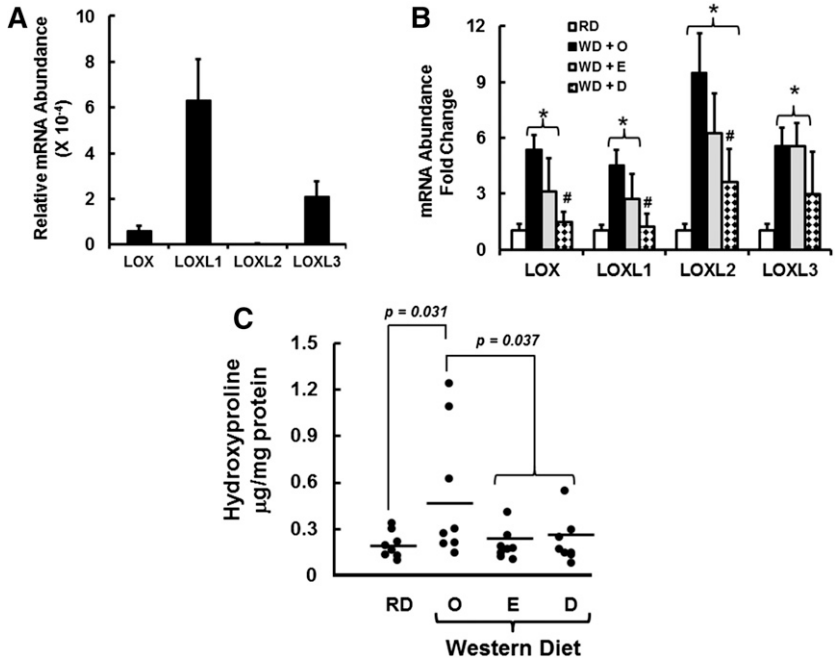

Fig. 5. Diet effects on hepatic expression of Lox and LoxL subtypes and hydroxyproline abundance. A: The relative expression of hepatic LOX and LOXL subtypes was quantified by qRT-PCR using liver RNA from mice fed the RD; cyclophilin was the reference transcript. The qRT-PCR primers are listed in supplementary Table 1. B: Effect of diet on LOX and LOXL subtype mRNA abundance. Results are expressed as mRNA abundance-fold change (mean ± SD; n = 8). $^{*}P \leq 0.05$ versus RD; $^{\#}P \leq 0.05$ versus WD + O. C: Hepatic hydroxyproline abundance was quantified as described in Materials and Methods and represented as µg hydroxyproline/mg protein (mean ± SD; n = 8). *P* values were calculated using Student's *t*-test.

acids used to treat cells; 18:1,ω9, 20:4,ω6, and 22:6,ω3 increased ~2-, 3-, and 5-fold, respectively. Treatment of cells with 20:4,ω6 increased LX2 cell levels of 22:4,ω6 and 22:5,ω6, whereas treatment of cells with DHA increased 20:5,ω3 and 22:5,ω3. The appearance of 22:4,ω6 and 22:5,ω6 in cells treated with 20:4,ω6 is due to elongation, desaturation, and peroxisomal β-oxidation activities in these cells. The appearance of 20:5,ω3 and 22:5,ω3 in DHA-treated cells is due to retro-conversion of 22:6,ω3 to 20:5,ω3, a peroxisome-dependent mechanism, and the elongation of 20:5,ω3 to 22:5,ω3 (61). We also show that LX2 cells express key enzymes involved in fatty acid synthesis and are capable of de novo lipogenesis and fatty acid elongation and desaturation of linoleic acid (18:2,ω6) and α-linolenic acid (18:3,ω3) to generate docosapentaenoic acid (22:5,ω6) and DHA (22:6,ω3), respectively (supplementary Fig. 2). In addition, other investigators have reported that LX2 and isolated primary rat stellate cells assimilate exogenous fatty acids into phospho- and neutral lipids (62). As such, LX2 cells have the capacity to synthesize

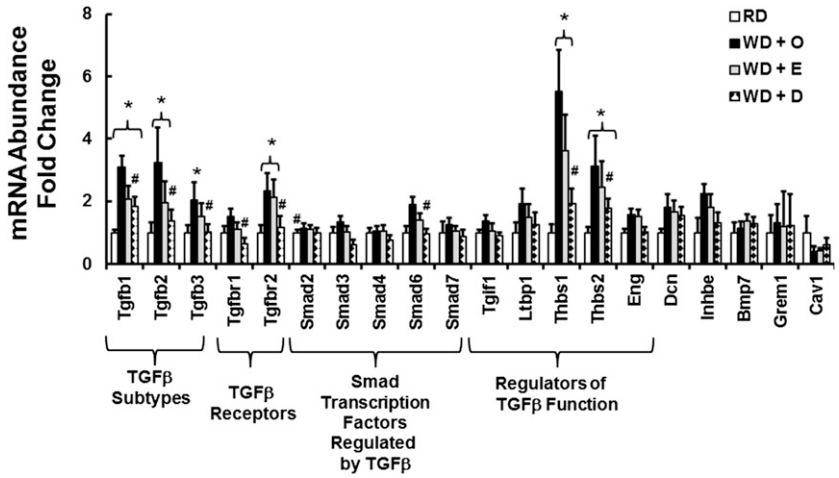

Fig. 6. Diet effects on expression of the TGFβ superfamily. Transcript abundance of proteins involved in TGFβ signaling was quantified using data from the qRT-PCR fibrosis array (Fig. 2). Results are represented as mRNA abundance-fold change (mean ± SD; n = 8). $^{*}P \leq 0.05$ versus RD; $^{\#}P \leq 0.05$ versus WD + O.

JOURNAL OF LIPID RESEARCH ASBMB

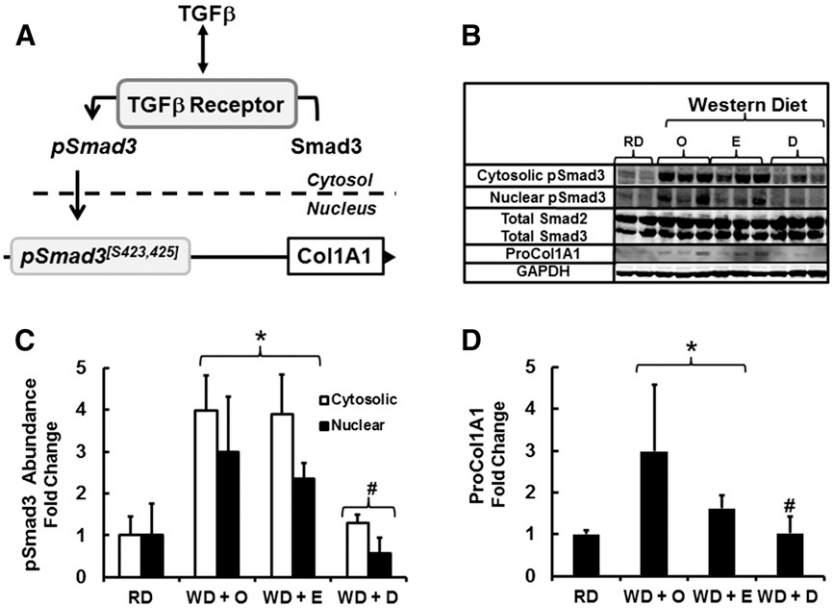

Fig. 7. Diet effects on Smad3 phosphorylation and Col1A1 precursor protein. Mouse liver cytosolic and nuclear extracts were prepared for immunoblotting as described (17). Antibodies used to detect total and phosphorylated Smad2 and -3 are listed in the Materials and Methods section. A: The pathway for TGFβ regulation of Col1A1 gene transcription (56–59). B: Representative immunoblot of total Smad 2, Smad3, phospho-Smad3, and proCol1A1. The loading control for phospho-Smad3 was total Smad3; while the loading control for proCol1A1 was GAPDH. The number of independent samples for each group was: RD, 2; WD + O, 3; WD + E, 3; WD + D, 3. C and D: Results are quantified for phospho-Smad3 (C) and proCol1A1 (D) and expressed as fold change (mean ± SD). $^{*}P \leq 0.05$ versus RD; $^{\#}P \leq 0.05$ versus WD + O.

fatty acids de novo and to transport exogenous fatty acids from the media into cells and metabolize these fatty acids.

To assess the impact of fatty acids on stellate cell function, LX2 cells were treated with TGFβ1 (100 pM, overnight) after prior fatty acid treatment, as described above. TGFβ treatment of LX2 cells induced Col1A1 expression 4-fold in vehicle-treated cells and cells pretreated with oleic acid (18:1,ω9) or arachidonic acid (20:4,ω6). DHA pretreatment, however, blocked TGFβ1 induction of Col1A1 mRNA. Thus, DHA has the capacity to act directly on human hepatic stellate cells to attenuate TGFβ1-mediated induction of Col1A1.

DISCUSSION

The goal of this report was to identify mechanisms that explain the differential effect of EPA and DHA on WD-induced hepatic fibrosis. This is highly relevant because dietary ω3 PUFAs are being evaluated as treatment strategies for NAFLD/NASH in children and adults (30–35, 63). Although these clinical studies show that dietary ω3 PUFAs reduce liver fat (30–37), some clinical trials have reported that ω3 PUFAs, like fish oil (36) or EPA-ethyl esters (37), fail to improve fibrosis scores associated with NASH. Our previous report established that DHA was more effective than EPA at attenuating WD-induced hepatic fat, inflammation, and fibrosis (17). Hepatic fibrosis in that study examined hepatic expression of three fibrosis gene expression markers (Col1A1, Timp1, and TGF-β1) and histology (i.e., trichrome staining of liver).

In this report, we have expanded our analysis of diet effects on hepatic fibrosis by quantifying 84 gene expression markers of fibrosis, four plasma markers linked to fibrosis, hepatic TGFβ-Smad signaling, and fatty acid effects on TGFβ signaling in human stellate (LX2) cells. Feeding $Ldlr^{-/-}$ mice the WD supplemented with DHA (WD + D), but not the WD + E diet, abrogated WD + O-induced accumulation of phospho-Smad3 in hepatic nuclei (Fig. 7). TGFβ is a major regulator of hepatic fibrosis (48). TGFβ binding to the TGFβ receptor increases Smad3 phosphorylation, and phospho-Smad3 migrates from the cytosol to the nucleus where it binds the Col1A promoter and induces transcription of the Col1A1 gene (55, 59). Although TGFβ signaling is operative in multiple hepatic cell types, including hepatocytes (64), the effect of WD and DHA on phospho-Smad3 correlates with changes in hepatic stellate cell expression of Col1A1 mRNA and proCol1A1 (Fig. 7). Moreover, we show that DHA acts directly on human LX2 stellate cells to block TGFβ1 induction of Col1A1 gene expression (Fig. 8). Taken together, these findings establish DHA as a regulator of TGFβ signaling and Col1A1 expression.

Our analysis revealed broad effects of the WD and $C_{20\text{-}22}$ ω3 PUFA on the expression of genes involved in fibrosis and TGFβ signaling (Fig. 2–6). Feeding mice the WD + O diet induced multiple components associated with TGFβ signaling, including several TGFβ subtypes (TGFβ1–3), a TGFβ receptor subunit (TGFβ-R2), and two thrombospondins (Thbs1 and Thbs2). Thbs1 and Thbs2 are expressed in macrophage, whereas Thbs2 is also expressed in endothelial cells (65, 66). Thbs1 induces TGFβ−dependent and TGFβ−independent fibrosis. DHA has been reported to

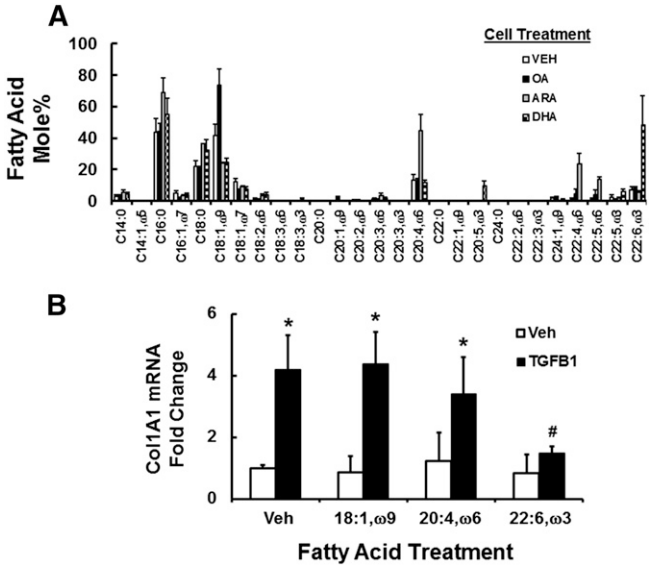

Fig. 8. TGFβ1 and DHA regulation of proCol1A1 expression in human LX2 stellate cells. LX2 cells were plated at ~10% confluence on plastic petri dishes in DMEM + 5% FCS and antibiotics. The next day, cells were treated with vehicle (Veh: fatty acid- and endotoxin-free BSA at 10 μM) or 25 μM fatty acids in BSA-containing media. Media was change every third day. This treatment enriches membrane lipids with exogenous fatty acids. A: Cells were harvested for fatty acid extraction and gas chromatographic quantitation. The results are presented as fatty acid, Mol% (mean ± range of two separate studies). B: Cells were treated with oleic acid (OA), arachidonic acid (ARA), or DHA as described above. After fatty acid pretreatment, cells were treated without or with 100 pM TGFβ1 overnight in the absence of fatty acids. Cells were harvested for RNA for qRT-PCR quantitation of proCol1A1 mRNA; hydroxymethylbilane synthase was the reference RNA. Results are presented as Col1A1 mRNA-fold change (mean ± SD; n = 3). $^{*}P \leq 0.05$ versus Veh; $^{\#}P \leq 0.05$ versus 18:1,ω9 + TGFβ.

suppress Thbs1 expression in adipose tissue (65). Thbs2, in contrast, attenuates fibrosis (67, 68). We are unaware of reports documenting effects of dietary PUFA on Thbs2 expression. The WD + D diet was more effective than the WD + E diet in attenuating WD + O induction of all TGFβ subtypes, both TGFβ subunits (R1 and R2), Smad6, and Thbs1 and Thbs2.

Our findings go beyond an earlier report by Chen et al. (69), who showed that DHA attenuated fibrosis in a rat bile duct ligation model for cholestatic liver injury. Although these investigators showed that DHA targeted TGFβ, NFκB, and Erk signaling, the authors did not assess effects of other fatty acids, Smad phosphorylation, and cytosolic-nuclear trafficking or TGFβ control in human hepatic stellate cells. Although cholestatic liver injury has a different etiology than diet-induced NASH in obese patients, these and other studies (70) suggest that DHA may have antifibrotic effects in liver and other tissues by controlling TGFβ signaling.

Regulators of hepatic fibrosis

Factors promoting diet-induced hepatic fibrosis are derived from multiple sources, including the gut (51) and multiple cell types, such as adipocytes (leptin), macrophages (TGFβ, PDGF, and IL1β), and T-cells (IL4, IL13, and TGFβ) that secret adipokines, growth factors, cytokines, and chemokines (52, 53). Hyperleptinemia, endotoxinemia, and increased plasma TNFα and TLR agonists are associated with hepatic fibrosis (49, 52). Supplementing the WD with EPA or DHA had no effect on WD-induced obesity or plasma levels of glucose, leptin, endotoxin, TNFα or TLR-4 agonist. The WD + D diet, however, attenuated WD-induced dyslipidemia (17) and TLR2 agonist (Fig. 1).

Although ω3 PUFA-containing WD diets reduce blood lipids, these diets significantly change the blood fatty acid profiles, leading to enrichment in $C_{20\text{-}22}$ ω3 PUFA and a decline in $C_{20\text{-}22}$ ω6 PUFA. The $C_{20\text{-}22}$ ω6 and the $C_{20\text{-}22}$ ω6 PUFA are precursors to proinflammatory and antiinflammatory bioactive lipids, respectively (71). Our studies establish that DHA can act directly on LX2 cells to regulate TGFβ1 control of Col1A1 expression (Fig. 8). This outcome does not exclude a role for other factors affecting stellate cell function. In fact, our previous (17) and current studies (supplementary Fig. 3) show WD + O effects on the expression of multiple hepatic chemokines [monocyte chemoattractant protein-1/Ccl2, Ccl3, Ccl12, and Cxcr4 (Ccl12 receptor)], cytokines (TNFα, IL1α, IL1β, and IL10), growth factors (PDGF-A, PDGF-B, and HGF), and transcription factors (Jun, Myc, and Stat1) linked to fibrosis. Moreover, we previously reported that the WD + O diet induced hepatic nuclear abundance of NFκB-p50 and NFκB-p65, whereas the WD + D (but not the WD + E) diet significantly lowered hepatic nuclear content of NFκB-p50 (17). Diet-induced changes in hepatic NFκB-p50 correlated with the hepatic abundance of downstream targets of TLR and NFκB, including cytokines and chemokines.

Because TLRs and cytokines are expressed in multiple hepatic cell types, we predict that the in vivo mechanism for DHA control of Col1A1 expression likely involves both direct effects of DHA on stellate cells (Fig. 8) and indirect effects mediated by changes in the function of Kupffer cells and macrophages and T-cells infiltrating the liver. Two factors support this hypothesis. First, the level of TGFβ1-mediated induction of Col1A1 in LX2 stellate cells is modest (4-fold) when compared with the nearly 20-fold induction of Col1A1 seen in vivo. Second, DHA is a pleiotropic mediator of cell function affecting multiple pathways, such as membrane composition as well as multiple cell signaling and transcription regulatory networks (29). In addition to stellate-macrophage interaction, hepatocyte-stellate cell interaction has been reported (72). As such, the LX2 cells can serve as a model to investigate how ω3 PUFAs regulate factors derived from hepatocytes and Kupffer cell/macrophage to control stellate cell function.

ECM remodeling enzymes

The progression and remission of fibrosis requires a balance in expression of ECM genes and enzymes that remodel the ECM. The WD induces expression of several hepatic collagen subtypes (Fig. 3) as well as enzymes involved in ECM remodeling, including metalloproteases (Mmp1a, Mmp2, and Mmp13), protease inhibitors [Timp1 and Timp2, serine protease inhibitors (serpine1

and serpinh1)], and enzymes involved in collagen cross-linking (Lox and LoxL1-3) (Figs. 4 and 5). Mmps and Timps are products of hepatocytes, leukocytes, Kupffer cells, and stellate/myofibrillar cells (16). A response favoring ECM removal will involve increased expression of Mmps, decreased Timp expression, decreased interaction of Timps with Mmps, and increased IL-10 and IL-13Ra2 (decoy receptor for IL13) expression (supplementary Fig. 3) (53). The WD, however, induced both metalloproteases and protease inhibitors involved in ECM remodeling, whereas $C_{20\text{-}22}$ ω3 PUFA attenuated this response. As such, the impact of ω3 PUFA on Mmp1a, Mmp2, and Mmp13 expression raises a concern for the capacity of these dietary lipids to promote remission of fibrosis in livers with preexisting fibrosis. Moreover, the WD + O diet induced IL-10, whereas the WD + D diet attenuated this response (supplementary Fig. 3). Although our study design was on prevention of diet-induced fibrosis, these concerted effects of DHA on factors involved in ECM removal raise the possibility that DHA may not be an effective NASH therapy that promotes remission of fibrosis. Further studies are required to quantify protein levels of Timps and Mmps, assess their activity, establish their subcellular localization, and examine protein-protein interaction. Such studies may reveal that $C_{20\text{-}22}$ ω3 PUFAs change the balance of ECM remodeling enzymes to favor removal of ECM.

Can ω3 PUFA be used to treat human NASH?

Our mouse studies provide strong evidence in support of the use of DHA in the prevention of NAFLD/NASH. Omega-3 PUFAs have well-defined effects on hepatic lipid metabolism and inflammation (29, 73), and more recently their effects on hepatic fibrosis have been noted (17, 28, 69). Although several human studies have provided evidence in support of using supplemental ω3 PUFAs to treat NAFLD (30–37), other studies suggest there may be limitations for their use in NASH treatment (36, 37). In trials using either fish oil or EPA-ethyl ester supplements, investigators report that ω3 PUFA supplements failed to improve fibrosis scores. Because DHA attenuates fibrosis in two separate rodent models of liver injury and fibrosis (i.e., WD-fed mice and rats with bile duct ligation) (17, 28, 69), failure of ω3 PUFAs to attenuate fibrosis in human clinical studies may be due to the type and dose of ω3 PUFAs used in the study. The finding that DHA suppressed TGF-β signaling and Col1A1 expression in mouse liver (Figs. 3 and 7) and human stellate cells (Fig. 8) suggests that DHA likely functions in humans.

DHA is the main ω3-PUFA accumulating in human and rodent tissues. Although α-linolenic acid and EPA are converted to DHA in humans, this process is insufficient for the accumulation of tissue levels of DHA needed to affect disease processes (74, 75). Humans and rodents retro-convert ingested DHA to EPA. In *Ldlr*$^{-/-}$ mice, for example, WD supplementation with DHA leads to a 30% and 500% increase in hepatic phospholipid DHA and EPA content, respectively (18). In contrast, phospholipid DHA levels do not increase in mice fed the WD supplemented with EPA. Moreover, the JELIS trial, a primary prevention trial for cardiovascular disease, clearly showed that feeding humans EPA did not increase blood DHA (74). In rodents, EPA and DHA suppress the expression of enzymes involved in PUFA synthesis (17). This mechanism involves the suppression of sterol regulatory element binding protein nuclear abundance (28), a key transcription factor regulating de novo lipogenesis and PUFA synthesis (29). As such, this mechanism lowers the capacity of cells to convert dietary C_{18}-PUFA precursors to $C_{20\text{-}22}$ ω3 and ω6 PUFAs. Because dietary DHA is retroconverted to EPA through a peroxisomal mechanism (61) and EPA is not well converted to DHA in vivo, DHA is a logical choice for usage in clinical trials.

In a recent double-blind, placebo-controlled trial, NAFLD patients received placebo or Lovaza™ at 4 g/d (~50:50 mix of EPA- and DHA-ethyl esters) for 15–18 months (35). When compared with the placebo-treated group, the Lovaza™-treated group showed a significant reduction in liver fat without a significant reduction in fibrosis scores. In our studies, $C_{20\text{-}22}$ ω3 PUFA in the WD + E or WD + D diets was used at 2% total energy. This dose of $C_{20\text{-}22}$ ω3 PUFA is comparable to the dose consumed by patients taking Lovaza™ to treat dyslipidemia (38). The dose used in our studies increased plasma $C_{20\text{-}22}$ ω3 PUFA in mice to levels seen in humans consuming 4–6 g/d of $C_{20\text{-}22}$ ω3 PUFA (39–41). We also used a combination of EPA and DHA to mimic Lovaza™ treatment (17). Whereas the overall $C_{20\text{-}22}$ ω3 PUFA dose was at 2% total energy, EPA and DHA were at 1% total energy each. The combination of EPA + DHA was less effective than using DHA alone at suppressing Col1A1 expression. As such, the preclinical prevention studies with *Ldlr*$^{-/-}$ mice suggest that DHA (at 4–6 g/d) may be more effective than EPA or fish oil at preventing diet-induced NASH and fibrosis in humans. A search of clinical trials (www.clinicaltrials.gov; query "NASH and DHA") yields three trials that are recruiting or active. The outcome of these studies may provide evidence in support of the use of dietary DHA in the prevention or treatment of diet-induced fibrosis.

Summary

This study identified mechanisms to explain the differential effects of EPA and DHA on WD-induced hepatic fibrosis. Feeding *Ldlr*$^{-/-}$ mice the WD induced changes in expression of multiple genes associated with hepatic inflammation and fibrosis. DHA, but not EPA, attenuated WD-induced hepatic fibrosis by targeting the TGFβ-Smad3-Col1A1 pathway. Moreover, DHA acted directly on human LX2 stellate cells to block TGFβ1-mediated induction of Col1A1. These outcomes establish DHA as a key regulator of TGFβ signaling and hepatic fibrosis.

REFERENCES

1. Angulo, P. 2002. Nonalcoholic fatty liver disease. *N. Engl. J. Med.* **346:** 1221–1231.
2. Chalasani, N., Z. Younossi, J. E. Lavine, A. M. Diehl, E. M. Brunt, K. Cusi, M. Charlton, and A. J. Sanyal. 2012. The diagnosis and management of non-alcoholic fatty liver disease: practice guideline

by the American Gastroenterological Association, American Association for the Study of Liver Diseases, and American College of Gastroenterology. *Gastroenterology.* **142:** 1592–1609.
3. Vernon, G., A. Baranova, and Z. M. Younossi. 2011. Systematic review: the epidemiology and natural history of non-alcoholic fatty liver disease and non-alcoholic steatohepatitis in adults. *Aliment. Pharmacol. Ther.* **34:** 274–285.
4. McCullough, A. J. 2006. Pathophysiology of nonalcoholic steatohepatitis. *J. Clin. Gastroenterol.* **40(Suppl 1):** S17–S29.
5. Prashanth, M., H. K. Ganesh, M. V. Vima, M. John, T. Bandgar, S. R. Joshi, S. R. Shah, P. M. Rathi, A. S. Joshi, H. Thakkar, et al. 2009. Prevalence of nonalcoholic fatty liver disease in patients with type 2 diabetes mellitus. *J. Assoc. Physicians India.* **57:** 205–210.
6. Soderberg, C., P. Stal, J. Askling, H. Glaumann, G. Lindberg, J. Marmur, and R. Hultcrantz. 2010. Decreased survival of subjects with elevated liver function tests during a 28-year follow-up. *Hepatology.* **51:** 595–602.
7. Ekstedt, M., L. E. Franzen, U. L. Mathiesen, L. Thorelius, M. Holmqvist, G. Bodemar, and S. Kechagias. 2006. Long-term follow-up of patients with NAFLD and elevated liver enzymes. *Hepatology.* **44:** 865–873.
8. Adams, L. A., J. F. Lymp, J. St Sauver, S. O. Sanderson, K. D. Lindor, A. Feldstein, and P. Angulo. 2005. The natural history of nonalcoholic fatty liver disease: a population-based cohort study. *Gastroenterology.* **129:** 113–121.
9. McCullough, A. J. 2004. The clinical features, diagnosis and natural history of nonalcoholic fatty liver disease. *Clin. Liver Dis.* **8:** 521–533 (viii.).
10. Sanyal, A. J., S. K. Yoon, and R. Lencioni. 2010. The etiology of hepatocellular carcinoma and consequences for treatment. *Oncologist.* **15(Suppl 4):** 14–22.
11. Cohen, J. C., J. D. Horton, and H. H. Hobbs. 2011. Human fatty liver disease: old questions and new insights. *Science.* **332:** 1519–1523.
12. Jiang, C. M., C. W. Pu, Y. H. Hou, Z. Chen, M. Alanazy, and L. Hebbard. 2014. Non alcoholic steatohepatitis a precursor for hepatocellular carcinoma development. *World J. Gastroenterol.* **20:** 16464–16473.
13. Oda, K., H. Uto, S. Mawaari, and A. Ido. 2015. Clinical features of hepatocellular carcinoma associated with nonalcoholic fatty liver disease: a review of human studies. *Clin. J. Gastroenterol.* In press.
14. Scalera, A., and G. Tarantino. 2014. Could metabolic syndrome lead to hepatocellular carcinoma via non-alcoholic fatty liver disease? *World J. Gastroenterol.* **20:** 9217–9228.
15. McCullough, A. J. 2011. Epidemiology of the metabolic syndrome in the USA. *J. Dig. Dis.* **12:** 333–340.
16. Duarte, S., Baber, J., Fujii, T., Coito, A.J. 2015. Matrix metalloproteases in liver injury, repair and fibrosis. *Matrix Biol.* **44–66C**: 147–159.
17. Depner, C. M., K. A. Philbrick, and D. B. Jump. 2013. Docosahexaenoic acid attenuates hepatic inflammation, oxidative stress, and fibrosis without decreasing hepatosteatosis in a Ldlr(−/−) mouse model of western diet-induced nonalcoholic steatohepatitis. *J. Nutr.* **143:** 315–323.
18. Depner, C. M., M. G. Traber, G. Bobe, K. M. Bohren, E. Morin-Kensicki, G. Milne, and D. B. Jump. 2013. A metabolomic analysis of omega-3 fatty acid mediated attenuation of western diet-induced non-alcoholic steatohepatitis in LDLR−/− mice. *PLoS One.* **8:** e83756.
19. Cordain, L., S. B. Eaton, A. Sebastian, N. Mann, S. Lindeberg, B. A. Watkins, J. H. O'Keefe, and J. Brand-Miller. 2005. Orgins and evolution of the western diet: health implications for the 21st century. *Am. J. Clin. Nutr.* **81:** 341–354.
20. Abdelmalek, M. F., A. Suzuki, C. Guy, A. Unalp-Arida, R. Colvin, R. J. Johnson, and A. M. Diehl. 2010. Increased fructose consumption is associated with fibrosis severity in patients with nonalcoholic fatty liver disease. *Hepatology.* **51:** 1961–1971.
21. Guturu, P., and A. Duchini. 2012. Etiopathogenesis of nonalcoholic steatohepatitis: role of obesity, insulin resistance and mechanisms of hepatotoxicity. *Int. J. Hepatol.* **2012:** 212865.
22. Wouters, K., P. J. van Gorp, V. Bieghs, M. J. Gijbels, H. Duimel, D. Lutjohann, A. Kerksiek, R. van Kruchten, N. Maeda, B. Staels, et al. 2008. Dietary cholesterol, rather than liver steatosis, leads to hepatic inflammation in hyperlipidemic mouse models of nonalcoholic steatohepatitis. *Hepatology.* **48:** 474–486.
23. Pagadala, M., T. Kasumov, A. J. McCullough, N. N. Zein, and J. P. Kirwan. 2012. Role of ceramides in nonalcoholic fatty liver disease. *Trends Endocrinol. Metab.* **23:** 365–371.
24. Harte, A. L., N. F. da Silva, S. J. Creely, K. C. McGee, T. Billyard, E. M. Youssef-Elabd, G. Tripathi, E. Ashour, M. S. Abdalla, H. M. Sharada, et al. 2010. Elevated endotoxin levels in non-alcoholic fatty liver disease. *J. Inflamm. (Lond).* **7:** 15.
25. Hooper, A. J., L. A. Adams, and J. R. Burnett. 2011. Genetic determinants of hepatic steatosis in man. *J. Lipid Res.* **52:** 593–617.
26. Dapito, D. H., A. Mencin, G. Y. Gwak, J. P. Pradere, M. K. Jang, I. Mederacke, J. M. Caviglia, H. Khiabanian, A. Adeyemi, R. Bataller, et al. 2012. Promotion of hepatocellular carcinoma by the intestinal microbiota and TLR4. *Cancer Cell.* **21:** 504–516.
27. Henao-Mejia, J., E. Elinav, C. Jin, L. Hao, W. Z. Mehal, T. Strowig, C. A. Thaiss, A. L. Kau, S. C. Eisenbarth, M. J. Jurczak, et al. 2012. Inflammasome-mediated dysbiosis regulates progression of NAFLD and obesity. *Nature.* **482:** 179–185.
28. Depner, C. M., M. Torres-Gonzalez, S. Tripathy, G. Milne, and D. B. Jump. 2012. Menhaden oil decreases high-fat diet-induced markers of hepatic damage, steatosis, inflammation, and fibrosis in obese Ldlr−/− mice. *J. Nutr.* **142:** 1495–1503.
29. Jump, D. B., S. Tripathy, and C. M. Depner. 2013. Fatty acid-regulated transcription factors in the liver. *Annu. Rev. Nutr.* **33:** 249–269.
30. Nobili, V., G. Bedogni, A. Alisi, A. Pietrobattista, P. Rise, C. Galli, and C. Agostoni. 2011. Docosahexaenoic acid supplementation decreases liver fat content in children with non-alcoholic fatty liver disease: double-blind randomised controlled clinical trial. *Arch. Dis. Child.* **96:** 350–353.
31. Sofi, F., I. Giangrandi, F. Cesari, I. Corsani, R. Abbate, G. F. Gensini, and A. Casini. 2010. Effects of a 1-year dietary intervention with n-3 polyunsaturated fatty acid-enriched olive oil on non-alcoholic fatty liver disease patients: a preliminary study. *Int. J. Food Sci. Nutr.* **61:** 792–802.
32. Bulchandani, D. G., J. S. Nachnani, A. Nookala, C. Naumovitch, B. Herndon, A. Molteni, T. Quinn, and L. M. Alba. 2010. Treatment with omega-3 fatty acids but not exendin-4 improves hepatic steatosis. *Eur. J. Gastroenterol. Hepatol.* **22:** 1245–1252.
33. Ishikawa, Y., M. Yokoyama, Y. Saito, M. Matsuzaki, H. Origasa, S. Oikawa, J. Sasaki, H. Hishida, H. Itakura, T. Kita, et al. 2010. Preventive effects of eicosapentaenoic acid on coronary artery disease in patients with peripheral artery disease. *Circ. J.* **74:** 1451–1457.
34. Kishino, T., H. Ohnishi, K. Ohtsuka, S. Matsushima, T. Urata, K. Watanebe, Y. Honda, Y. Mine, M. Matsumoto, K. Nishikawa, et al. 2011. Low concentrations of serum n-3 polyunsaturated fatty acids in non-alcoholic fatty liver disease patients with liver injury. *Clin. Chem. Lab. Med.* **49:** 159–162.
35. Scorletti, E., L. Bhatia, K. G. McCormick, G. F. Clough, K. Nash, L. Hodson, H. E. Moyses, P. C. Calder, C. D. Byrne; WELCOME study. 2014. Effects of purified eicosapentaenoic and docosahexaenoic acids in non-alcoholic fatty liver disease: results from the WELCOME study. *Hepatology.* **60:** 1211–1221.
36. Argo, C. K., J. T. Patrie, C. Lackner, T. D. Henry, E. E. de Lang, A. L. Weltman, N. L. Shah, A. M. Al-Osaimi, P. Pramoonjago, S. Jayakumar, et al. 2015. Effects of n-3 fish oil on metabolic and histological parameters in NASH: a double-blind, randomized, placebo-controlled trial. *J. Hepatol.* **62:** 190–197.
37. Sanyal, A. J., M. F. Abdelmalek, A. Suzuki, O. W. Cummings, and M. Chojkier. 2014. No significant effects of ethyl-eicosapentaenoic acid on histologic features of nonalcoholic steatohepatitis in a phase 2 trial. *Gastroenterology.* **147:** 377–384.
38. Barter, P., and H. N. Ginsberg. 2008. Effectiveness of combined statin plus omega-3 fatty acid therapy for mixed dyslipidemia. *Am. J. Cardiol.* **102:** 1040–1045.
39. Di Stasi, D., R. Bernasconi, R. Marchioli, R. M. Marfisi, G. Rossi, G. Tognoni, and M. T. Tacconi. 2004. Early modification of fatty acid composition in plasma phospholipids, platelets and mononucleates of healthy volunteers after low doses of n-3 PUFA. *Eur. J. Clin. Pharmacol.* **60:** 183–190.
40. Superko, H. R., S. M. Superko, K. Nasir, A. Agatston, and B. C. Garrett. 2013. Omega-3 fatty acid blood levels. Clinical significance and controversy. *Circulation.* **128:** 2154–2161.
41. Lockyer, S., M. Tzanetou, A. L. Carvalho-Wells, J. G. Jackson, A. M. Minihane, and J. A. Lovegrove. 2012. STAT gene dietary model to implement diets of differing fat composition in prospectively genotyped groups (apoE) using commercially available foods. *Br. J. Nutr.* **108:** 1705–1713.
42. Tripathy, S., M. Torres-Gonzalez, and D. B. Jump. 2010. Elevated hepatic fatty acid elongase-5 activity corrects dietary fat-induced hyperglycemia in obese C57BL/6J mice. *J. Lipid Res.* **51:** 2642–2654.

43. Xu, L., A. Y. Hui, E. Albanis, M. J. Arthur, S. M. O'Byrne, W. S. Blaner, P. Mukherjee, S. L. Friedman, and F. J. Eng. 2005. Human hepatic stellate cell lines, LX-1 and LX-2: new tools for the analysis of hepatic fibrosis. *Gut.* **54:** 142–151.
44. Weiskirchen, R., J. Weimer, S.K. Meurer, A. Kron, B. Seipel, I. Vater, N. Arnold, R. Siebert, L. Xu, S. L. Friedman, and C. Bergmann, C. 2013. Genetic characteristics of the human hepatic stellate cell line LX-2. *PLoS One.* **8:** e75692.
45. Tripathy, S., K. A. Lytle, R. D. Stevens, J. R. Bain, C. B. Newgard, A. S. Greenberg, L-S. Huang, and D. B. Jump. 2014. Fatty acid elongase-5 (Elovl5) regulates hepatic triglyceride catabolism in obese C57BL/6J mice. *J. Lipid Res.* **55:** 1448–1464.
46. Jump, D. B., M. Torres-Gonzalez, and L. K. Olson. 2011. Soraphen A, an inhibitor of acetyl CoA carboxylase activity, interferes with fatty acid elongation. *Biochem. Pharmacol.* **81:** 649–660.
47. Seki, E., S. De Minicis, C. H. Osterreicher, J. Kluwe, Y. Osawa, D. A. Brenner, and R. F. Schwabe. 2007. TLR4 enhances TGF-beta signaling and hepatic fibrosis. *Nat. Med.* **13:** 1324–1332.
48. Schuppan, D., Y. O. Kim. 2013. Evolving therapies for liver fibrosis. *J. Clin. Invest.* **123:** 1887–1901.
49. Cengiz, M., S. Ozenirler, and S. Elbeg. 2015. Role of serum toll-like receptors 2 and 4 in non-alcoholic steatohepatitis and liver fibrosis. *J. Gastroenterol. Hepatol.* **30:** 1190–1196.
50. Roh, Y. S., and E. Seki. 2013. Toll-like receptors in alcoholic liver disease, non-alcoholic steatohepatitis and carcinogenesis. *J. Gastroenterol. Hepatol.* **28(Suppl 1):** 38–42.
51. Beutler, B. 2002. TLR4 as the mammalian endotoxin sensor. *Curr. Top. Microbiol. Immunol.* **270:** 109–120.
52. Saxena, N. K., and F. A. Anania. 2015. Adipocytokines and hepatic fibrosis. *Trends Endocrinol. Metab.* **26:** 153–161.
53. Barron, L., and T. A. Wynn. 2011. Fibrosis is regulated by Th2 and Th17 responses and by dynamic interactions between fibroblasts and macrophage. *Am. J. Physiol. Gastrointest. Liver Physiol.* **300:** G723–G728.
54. Perepelyuk, M., M. Terajima, A. Y. Wang, P. C. Georges, P. A. Janmey, M. Yamauchi, and R. G. Wells. 2013. Hepatic stellate cells and portal fibrosis are the major cellular sources of collagens and lysyl oxidases in normal liver and early after injury. *Am. J. Physiol. Gastrointest. Liver Physiol.* **304:** G605–G614.
55. Massague, J. 2012. TGF-β signalling in context. *Nat. Rev. Mol. Cell Biol.* **13:** 616–630.
56. Akhurst, R. J., and A. Hata. 2012. Targeting the TGF-β signalling pathway in disease. *Nat. Rev. Drug Discov.* **11:** 790–811.
57. Han, J., C. A. Alverez-Breckenridge, Q-E. Wang, and J. Yu. 2015. TGF-β signaling and its targeting for glioma treatment. *Am. J. Cancer Res.* **5:** 945–955.
58. Murata, M., K. Yoshida, T. Yamaguchi, and K. Matsuzaki. 2014. Linker phosphorylation of Smad3 promotes fibro-carcinogenesis in chronic viral hepatitis of hepacellular carcinoma. *World J. Gastroenterol.* **20:** 15018–15027.
59. Verrecchia, F., M-L. Chu, and A. Mauviel. 2001. Identification of novel TGF-β/Smad gene targets in dermal fibroblast using a combined cRNA microarray/promoter transactivation approach. *J. Biol. Chem.* **276:** 17058–17062.
60. Nyati, S., K. Schinske-Sebolt, S. Pitchiaya, K, Chekhovskiy, A. Chator, N. Chaudhry, J. Dosch, M. E. Van Dort, S. Varambally, C. Kumar-Sinha, et al. 2015. The kinase activity of the Ser/Thr kinase Bub1 promotes TGF-β signaling. *Sci. Signal.* **8:** ra1.
61. Sprecher, H. 2000. Metabolism of highly unsaturated n-3 and n-6 fatty acids. *Biochim. Biophys. Acta.* **1486:** 219–231.
62. Tuohetahuntila, M., B. Spee, H. S. Kruitwagen, R. Wubbolts, J. F. Brouwers, C. H. van de Lest, M. R. Molenaar, M. Houweling, J. B. Helms, and A. B. Vaandrager. 2015. Role of long-chain acyl-CoA synthetase 4 in formation of polyunsaturated lipid species in hepatic stellate cells. *Biochim. Biophys. Acta.* **1851:** 220–230.
63. Parker, H. M., N. A. Johnson, C. A. Burdon, J. S. Cohn, H. T. O'Connor, and J. George. 2012. Omega-3 supplementation and non-alcoholic fatty liver disease: a systematic review and meta-analysis. *J. Hepatol.* **56:** 944–951.
64. Moreno-Caceres, J., L. Caja, J. Mainez, R. Mayoral, P. Martin-Sanz, R. Moreno-VIcente, M. A. del Pozo, S. Dooley, G. Egea, and I. Fabregat. 2014. Caveolin-1 is required for TGFβ-induced transactivation of the EGF receptor pathway in hepatocytes through the activation of the metalloprotease TACD/ADAM17. *Cell Death Dis.* **5:** e1326.
65. Finlin, B. S., B. Zhu, C. P. Starnes, R. E. McGehee, Jr., C. A. Peterson, and P. A. Kern. 2013. Regulation of thrombospondin-1 expression in alternatively activated macrophage and adipocytes: role of cellular crosstalk and omega-3 fatty acids. *J. Nutr. Biochem.* **24:** 1571–1579.
66. Park, Y. W., Y. M. Kang, J. Butterfield, M. Detmar, J. J. Goronzy, and C. M. Weyand. 2004. Thrombospondin 2 functions as an endogenous regulator of angiogenesis and inflammation in rheumatoid arthritis. *Am. J. Pathol.* **165:** 2087–2098.
67. Masli, S., N. Sheibani, C. Cursiefen, and J. Zieske. 2014. Matricellular protein thrombospondins: influence on ocular angiogenesis, wound healing and immuneregulation. *Curr. Eye Res.* **39:** 759–774.
68. Kim, D. J., E. D. Christofidou, D. R. Keene, M. H. Milde, and J. C. Adams. 2015. Inter-molecular interactions of thrombospondins drive their accumulation in extracellular matrix. *Mol. Biol. Cell.* In press.
69. Chen, W-Y., S-Y. Lin, H-C. Pan, S-L. Liao, Y-H. Chuang, Y-J. Yen, S-Y. Lin, and C-J. Chen. 2012. Beneficial effect of docosahexaenoic acid on cholestatic liver injury in rats. *J. Nutr. Biochem.* **23:** 252–264.
70. Zhao, H., Y. Chan-Li, S. L. Collins, Y. Zhang, R. W. Hallowell, W. Mitzner, and M. R. Horton. 2014. Pulmonary delivery of docosahexaenoic acid mitigates bleomycin-induced pulmonary fibrosis. *BMC Pulm Med* **14:** 64.
71. Calder, P. C. 2015. Marine omega-3 fatty acids and inflammatory processes: effects, mechanisms and clinical relevance. *Biochim. Biophys. Acta.* **1851:** 469–484.
72. Giraudi, P. J., V. J. Barbero Becerra, V. Marin, N. C. Chavez-Tapia, C. Tiribelli, and N. Rosso. 2015. The importance of the interaction between hepatocyte and hepatic stellate cells in fibrogenesis induced fatty accumulation. *Exp. Mol. Pathol.* **98:** 85–92.
73. Calder, P. C. 2012. Mechanisms of action of (n-3) fatty acids. *J. Nutr.* **142:** 592S–599S.
74. Itakura, H., M. Yokoyama, M. Matsuzaki, Y. Saito, H. Origasa, Y. Ishikawa, S. Oikawa, J. Sasaki, H. Hishida, T. Kita, et al. 2011. Relationships between plasma fatty acid composition and coronary artery disease. *J. Atheroscler. Thromb.* **18:** 99–107.
75. Jump, D. B., C. M. Depner, and S. Tripathy. 2012. Omega-3 fatty acid supplementation and cardiovascular disease. *J. Lipid Res.* **53:** 2525–2545.

Supplementary Data

Supplementary Tables

Table 1S: qRT-PCR Primers

Mouse		Accession#	Forward Primer	Reverse Primer
Collagen1A1	Col1A1	NM_007742.3	TAGGCCATTGTGTATGCAGC	ACATGTTCAGCTTTGTGGACC
Collagen1A2	Col1A2	NM_007743.2	GTCCTAGTCGATGGCTGCTC	AGCACCACCAATGTCCAGAG
Collagen 4A1	Col4A1	NM_009931.2	TTTGGCTCGCCACCATAGAG	GCAGAGGCGAGCATCATAGT
Collagen7A1	Col7A1	NM_007738.3	ACCGCATCTTCTGTTGAGCA	TTCCAAGCCACTCTCACGAC
Sm. muscle Actin	Acta2	NM_007392.2	AAGCCCAGCCAGTCGCTGTCA	AGCCCAGAGCCATTGTCGCA
Lysyl Oxidase	Lox	NM_010728.3	GGGCCAGAACGGCTTGTGTA	TCTGGGAAAGCGCACAGAGT
Lox-Like-1	LoxL1	NM_010729.3	TGTGGGGCTGGCCATGTAAG	AGGACAGGATGGCTCTTCGC
Lox-Like-2	LoxL2	NM_033325.2	AAGTGCAGGAGCCGCTATGA	TGCCAAAGCTCGGATGGGAT
Lox-Like-3	LoxL3	NM_013586.4	CAGTGTGTGGTATTGCTGCCC	TCTGAGAAACCGGGAAGGCG
Cyclophilin		NM_008907	CTTCTTGCTGGTCTTGCCATTCCT	GATGGCAAGCATGTGGTCTTTG
Human				
Collagen1A1	Col1A1	NM_000088.3	AATGGTGCTCCTGGTATTGC	ACCAGGTTCACCGCTGTTAC
Hydroxy methylbilane Synthase	HMBS	NM_000190.3	TCTGCGGAGACCAGGAGTCA	GTAGGCTGTGTGTGGGTGC

Table 2S: MOUSE FIBROSIS ARRAY GENE TABLE

Unigene	GeneBank	Symbol	Description	Gene Name
Mm.213025	NM_007392	**Acta2**	Actin, alpha 2, smooth muscle, aorta	0610041G09Rik, Actvs, SMalphaA, a-SMA, alphaSMA
Mm.301626	NM_007428	**Agt**	Angiotensinogen (serpin peptidase inhibitor, clade A, member 8)	AI265500, AngI, AngII, Aogen, Serpina8
Mm.6645	NM_009652	**Akt1**	Thymoma viral proto-oncogene 1	Akt, PKB, PKB, Akt, PKBalpha, Rac
Mm.257460	NM_009741	**Bcl2**	B-cell leukemia/lymphoma 2	AW986256, Bcl-2, C430015F12Rik, D630044D05Rik, D830018M01Rik
Mm.392150	NM_007557	**Bmp7**	Bone morphogenetic protein 7	OP1
Mm.28278	NM_007616	**Cav1**	Caveolin 1, caveolae protein	Cav, Cav-1
Mm.4686	NM_011330	**Ccl11**	Chemokine (C-C motif) ligand 11	Scya11, eotaxin
Mm.867	NM_011331	**Ccl12**	Chemokine (C-C motif) ligand 12	MCP-5, Scya12
Mm.1282	NM_011337	**Ccl3**	Chemokine (C-C motif) ligand 3	AI323804, G0S19-1, LD78alpha, MIP-1alpha, MIP1-(a), MIP1-alpha, Mip1a, Scya3
Mm.6272	NM_009915	**Ccr2**	Chemokine (C-C motif) receptor 2	Cc-ckr-2, Ccr2a, Ccr2b, Ckr2, Ckr2a, Ckr2b, Cmkbr2, mJe-r
Mm.439656	NM_009883	**Cebpb**	CCAAT/enhancer binding protein (C/EBP), beta	C, EBPbeta, CRP2, IL-6DBP, LAP, LIP, NF-IL6, NF-M, Nfil6
Mm.277792	NM_007743	**Col1a2**	Collagen, type I, alpha 2	AA960264, AI325291, Col1a-2, Cola-2, Cola2, oim
Mm.249555	NM_009930	**Col3a1**	Collagen, type III, alpha 1	AW550625, Col3a-1, MMS10-W, Ms10w, mKIAA4231
Mm.390287	NM_010217	**Ctgf**	Connective tissue growth factor	Ccn2, Fisp12, Hcs24, fisp-12
Mm.1401	NM_009911	**Cxcr4**	Chemokine (C-X-C motif) receptor 4	CD184, Cmkar4, LESTR, PB-CKR, PBSF, SDF-1, Sdf1r
Mm.56769	NM_007833	**Dcn**	Decorin	DC, DSPG2, PG40, PGII, PGS2, SLRR1B, mDcn
Mm.14543	NM_010104	**Edn1**	Endothelin 1	ET-1, preproET
Mm.252481	NM_010113	**Egf**	Epidermal growth factor	AI790464
Mm.225297	NM_007932	**Eng**	Endoglin	AI528660, AI662476, CD105, Endo, S-endoglin
Mm.3355	NM_010177	**Fasl**	Fas ligand (TNF superfamily, member 6)	APT1LG1, CD178, CD95-L, CD95L, Fas-L, Faslg, Tnfsf6, gld
Mm.166318	NM_011824	**Grem1**	Gremlin 1	Cktsf1b1, Drm, Grem, ld
Mm.267078	NM_010427	**Hgf**	Hepatocyte growth factor	C230052L06Rik, HGF, SF, NK1, NK2, SF, HGF
Mm.240327	NM_008337	**Ifng**	Interferon gamma	IFN-g, Ifg
Mm.874	NM_010548	**Il10**	Interleukin 10	CSIF, Il-10
Mm.1284	NM_008355	**Il13**	Interleukin 13	Il-13
Mm.368330	NM_008356	**Il13ra2**	Interleukin 13 receptor, alpha 2	CD213a2
Mm.15534	NM_010554	**Il1a**	Interleukin 1 alpha	Il-1a
Mm.222830	NM_008361	**Il1b**	Interleukin 1 beta	IL-1beta, Il-1b
Mm.276360	NM_021283	**Il4**	Interleukin 4	BSF-1, Il-4
Mm.4461	NM_010558	**Il5**	Interleukin 5	Il-5
Mm.274846	NM_010562	**Ilk**	Integrin linked kinase	AA511515, ESTM24
Mm.3510	NM_008382	**Inhbe**	Inhibin beta E	-
Mm.317280	NM_001033228	**Itga1**	Integrin alpha 1	CD49A, E130012M19Rik, Vla1
Mm.5007	NM_008396	**Itga2**	Integrin alpha 2	CD49B, DX5
Mm.57035	NM_013565	**Itga3**	Integrin alpha 3	AA407068, CD49C, GAPB3
Mm.227	NM_008402	**Itgav**	Integrin alpha V	1110004F14Rik, 2610028E01Rik, CD51, D430040G12Rik
Mm.263396	NM_010578	**Itgb1**	Integrin beta 1 (fibronectin receptor beta)	4633401G24Rik, AA409975, AA960159, CD29, ENSMUSG00000051907, Fnrb, Gm9863, gpIIa
Mm.87150	NM_016780	**Itgb3**	Integrin beta 3	CD61, GP3A, INGRB3
Mm.6424	NM_010580	**Itgb5**	Integrin beta 5	AA475909, AI874634, ESTM23, [b]-5, [b]5, [b]5A, [b]5B, beta-5, beta5
Mm.98193	NM_021359	**Itgb6**	Integrin beta 6	2210409C20Rik, 4831415H04Rik
Mm.217000	NM_177290	**Itgb8**	Integrin beta 8	4832412O06Rik
Mm.275071	NM_010591	**Jun**	Jun oncogene	AP-1, Junc, c-jun
Mm.488403	NM_010728	**Lox**	Lysyl oxidase	AI893619, TSC-160, rrg
Mm.269747	NM_019919	**Ltbp1**	Latent transforming growth factor beta binding protein 1	9430031G15Rik, 9830146M04, Ltbp-1, Tgfb, b2b1000Clo
Mm.5022	NM_008607	**Mmp13**	Matrix metallopeptidase 13	Clg, MMP-13, Mmp1
Mm.486486	NM_008608	**Mmp14**	Matrix metallopeptidase 14 (membrane-inserted)	AI325305, MT-MMP-1, MT1-MMP, sabe

Mm.156952	NM_032006	**Mmp1a**	Matrix metallopeptidase 1a (interstitial collagenase)	Mcol-A, Mcola
Mm.29564	NM_008610	**Mmp2**	Matrix metallopeptidase 2	Clg4a, GelA, MMP-2
Mm.4993	NM_010809	**Mmp3**	Matrix metallopeptidase 3	SLN-1, SLN1, STR-1, Stmy1, Str1
Mm.16415	NM_008611	**Mmp8**	Matrix metallopeptidase 8	BB138268
Mm.4406	NM_013599	**Mmp9**	Matrix metallopeptidase 9	AW743869, B, MMP9, Clg4b, MMP-9, pro-MMP-9
Mm.2444	NM_010849	**Myc**	Myelocytomatosis oncogene	AU016757, Myc2, Niard, Nird, bHLHe39
Mm.256765	NM_008689	**Nfkb1**	Nuclear factor of kappa light polypeptide gene enhancer in B-cells 1, p105	NF-KB1, NF-kappaB, NF-kappaB1, p105, p50, p50, p105
Mm.2675	NM_008808	**Pdgfa**	Platelet derived growth factor, alpha	-
Mm.144089	NM_011057	**Pdgfb**	Platelet derived growth factor, B polypeptide	PDGF-B, Sis
Mm.154660	NM_008872	**Plat**	Plasminogen activator, tissue	AU020998, AW212668, D8Ertd2e, tPA
Mm.4183	NM_008873	**Plau**	Plasminogen activator, urokinase	u-PA, uPA
Mm.971	NM_008877	**Plg**	Plasminogen	AI649309, Pg
Mm.439692	NM_009243	**Serpina1a**	Serine (or cysteine) peptidase inhibitor, clade A, member 1a	Aat-2, Aat2, Dom1, PI1, Spi1-1, Spi1-3
Mm.250422	NM_008871	**Serpine1**	Serine (or cysteine) peptidase inhibitor, clade E, member 1	PAI-1, PAI1, Planh1
Mm.22708	NM_009825	**Serpinh1**	Serine (or cysteine) peptidase inhibitor, clade H, member 1	BERF-1, Cbp1, Cbp2, Hsp47, J6, Serpinh2, gp46
Mm.490934	NM_010754	**Smad2**	MAD homolog 2 (Drosophila)	7120426M23Rik, Madh2, Madr2, Smad-2, mMad2
Mm.7320	NM_016769	**Smad3**	MAD homolog 3 (Drosophila)	AU022421, Madh3
Mm.100399	NM_008540	**Smad4**	MAD homolog 4 (Drosophila)	AW743858, D18Wsu70e, DPC4, Madh4
Mm.325757	NM_008542	**Smad6**	MAD homolog 6 (Drosophila)	Madh6, b2b390Clo
Mm.34407	NM_001042660	**Smad7**	MAD homolog 7 (Drosophila)	Madh7
Mm.2093	NM_011427	**Snai1**	Snail homolog 1 (Drosophila)	AI194338, Sna, Sna1, Snail, Snail1
Mm.4618	NM_013672	**Sp1**	Trans-acting transcription factor 1	1110003E12Rik, AA450830, AI845540, Sp1-1
Mm.487336	NM_009283	**Stat1**	Signal transducer and activator of transcription 1	2010005J02Rik, AA408197
Mm.121721	NM_009284	**Stat6**	Signal transducer and activator of transcription 6	-
Mm.248380	NM_011577	**Tgfb1**	Transforming growth factor, beta 1	TGF-beta1, TGFbeta1, Tgfb, Tgfb-1
Mm.18213	NM_009367	**Tgfb2**	Transforming growth factor, beta 2	BB105277, Tgf-beta2, Tgfb-2
Mm.3992	NM_009368	**Tgfb3**	Transforming growth factor, beta 3	Tgfb-3
Mm.197552	NM_009370	**Tgfbr1**	Transforming growth factor, beta receptor I	ALK5, AU017191, Alk-5, TbetaR-I, TbetaRI
Mm.172346	NM_009371	**Tgfbr2**	Transforming growth factor, beta receptor II	1110020H15Rik, AU042018, DNIIR, RIIDN, TBR-II, TbetaR-II, TbetaRII
Mm.101034	NM_009372	**Tgif1**	TGFB-induced factor homeobox 1	AA959811, AI462167, Tgif
Mm.4159	NM_011580	**Thbs1**	Thrombospondin 1	TSP-1, TSP1, Thbs-1, tbsp1
Mm.26688	NM_011581	**Thbs2**	Thrombospondin 2	TSP2, Thbs-2
Mm.8245	NM_011593	**Timp1**	Tissue inhibitor of metalloproteinase 1	Clgi, TIMP-1, Timp
Mm.206505	NM_011594	**Timp2**	Tissue inhibitor of metalloproteinase 2	D11Bwg1104e, Timp-2
Mm.4871	NM_011595	**Timp3**	Tissue inhibitor of metalloproteinase 3	Timp-3
Mm.255607	NM_080639	**Timp4**	Tissue inhibitor of metalloproteinase 4	TIMP-4
Mm.1293	NM_013693	**Tnf**	Tumor necrosis factor	DIF, TNF-a, TNF-alpha, TNFSF2, TNFalpha, Tnfa, Tnfsf1a
Mm.282184	NM_009505	**Vegfa**	Vascular endothelial growth factor A	Vegf, Vpf
Mm.391967	NM_007393	**Actb**	Actin, beta	Actx, E430023M04Rik, beta-actin
Mm.163	NM_009735	**B2m**	Beta-2 microglobulin	Ly-m11, beta2-m, beta2m
Mm.304088	NM_008084	**Gapdh**	Glyceraldehyde-3-phosphate dehydrogenase	Gapd
Mm.3317	NM_010368	**Gusb**	Glucuronidase, beta	AI747421, Gur, Gus, Gus-r, Gus-s, Gus-t, Gus-u, Gut, asd, g
Mm.2180	NM_008302	**Hsp90ab1**	Heat shock protein 90 alpha (cytosolic), class B member 1	90kDa, AL022974, C81438, Hsp84, Hsp84-1, Hsp90, Hspcb
N/A	SA_00106	**MGDC**	Mouse Genomic DNA Contamination	MIGX1B

Supplementary Data

Figure Legends:

Figure 1S. Activation of TLR2 and TLR4 using authentic ligands.

Hek-Blue^{TM}mTLR2 and Hek-blue^{TM}mTLR4 cells (Invivogen) were treated with PAM3CSK4 and LPS-B5, TLR2 and TLR4 agonist, respectively, overnight as described in Materials and Methods and Fig. 1. NFκB activation was quantified by absorbance at 620 nm.

Figure 2S. Assessment of fatty acid synthesis in LX2 human stellate cells.

Panels A and B: The relative abundance of mRNAs encoding proteins involved in *de novo* lipogenesis [DNL] (acetyl CoA carboxylase-1 [ACC1], fatty acid synthase [FASN]), fatty acid elongation (Elovl2, Elovl5) and desaturation (FADS1, FADS2); and two transcription factors (SREBP1a, SREBP1c) controlling expression of these enzymes was quantified by qRTPCR and RNA from human hepatoma (HepG2) and stellate (LX2) cells as described previously (1). The results are reported as Relative mRNA abundance, mean $\pm$ SD, N=3. **Panel C:** Confluent LX2 wells were treated with ^{14}C-acetate, ^{14}C-linoleate or ^{14}C-α-linoleate for 6 hours as described previously (1, 2). The labeling of cells was terminated by treatment with 0.4 M KOH in 80% methanol to saponify lipid. The recovered ^{14}C-labeled fatty acids were separated by RP-HPLC and radioactivity was quantified using an in-line β-scintillation counter. Results are represented as % Distribution of ^{14}C-fatty acids. Results are representative of 2 separate studies.

This analysis compared the level of expression of enzymes involved in DNL (ACC1, FASN), elongation and desaturation (Elovl2, Elovl5, FADS1, FADS2) and 2 transcription factors (SREBP1 & 2) involved in fatty acid synthesis in HepG2 (human hepatoma cells) and LX2 cells. While both HepG2 and LX2 cells express key enzymes involved in DNL, elongation and desaturation, levels of expression of these enzymes is different in the two cell types. HepG2 cells appear to have the high capacity for DNL, while LX2 cells may have higher capacity for long chain fatty acid elongation and desaturation. The capacity of HepG2 cells to carry out DNL, elongate and de-saturate fatty acids was previously reported

(1). To verify the capacity of LX2 cells to carry out fatty acid metabolism, cells were treated with ^{14}C-precursors to long chain fatty acids, i.e., acetate, linoleate and α-linolenate. LX2 cells convert ^{14}C-acetate to $C_{16\text{-}18}$ saturated (18:0) and monounsaturated fatty acids (16:1,ω7). Note that 16:0, 18:1,ω7 and 18:1,ω9 co-migrate in the RP-HPLC. ^{14}C-linoleate was converted to $C_{18\text{-}22}$ ω6 PUFA and ^{14}C-α-linolenate was converted to $C_{18\text{-}22}$ ω3 PUFA. Thus, LX2 cells have the capacity to synthesize fatty acids *de novo,* elongate and de-saturate essential fatty acids and modify fatty acids by peroxisomal β-oxidation, i.e., converted exogenous DHA to EPA, see **Fig. 8.**

Figure 3S: Diet effects on expression of the hepatic chemokines & cytokines, growth factors and transcription factors.

Transcript abundance of proteins encoding chemokines and cytokines (**Panel A**), growth factors (**Panel B**) and transcription factors (**Panel C**) was quantified using data from the qRTPCR fibrosis array data described in **Fig. 2**. Results are represented as mRNA Abundance-Fold Change, mean $\pm$ SD, n=8; *, *$p \leq 0.05$ versus RD; #, $p \leq 0.05$ versus WD + O.*

Literature cited.

1. Jump, D. B., M. Torres-Gonzalez, and L. K. Olson. 2011. Soraphen A, an inhibitor of acetyl CoA carboxylase activity, interferes with fatty acid elongation. *Biochem Pharmacol* **81**: 649-660.
2. Tripathy, S., Lytle, K.A., Stevens, R.D., Bain, J.R., Newgard, C.B., Greenberg, A.S., Huang, L-S., and Jump, D.B 2014. Fatty acid elongase-5 (Elovl5) regulates hepatic triglyceride catabolism in obese C57BL/6J mice *J Lipid Res* **55**: 1448-1464.

Supplement: Fig. 1S

A.

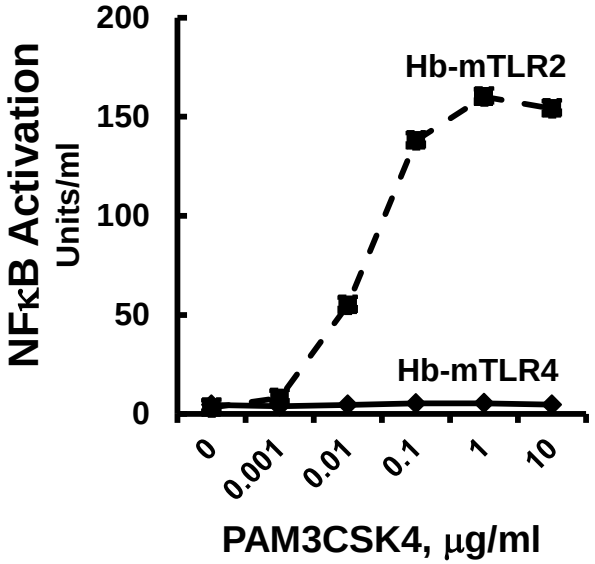

B.

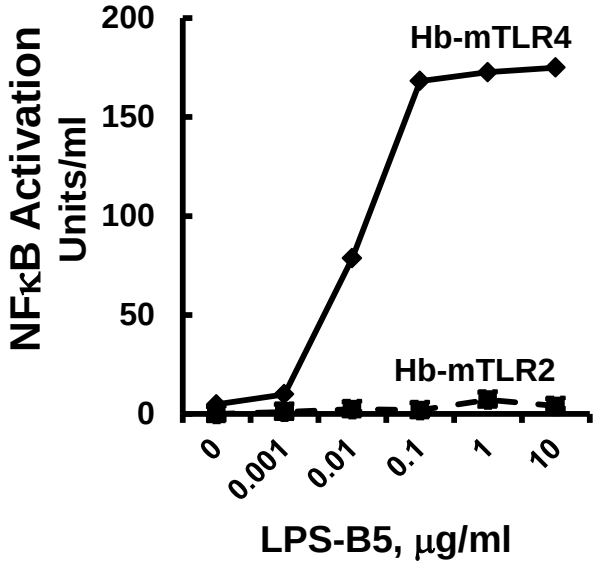

Supplement: Fig. 2S

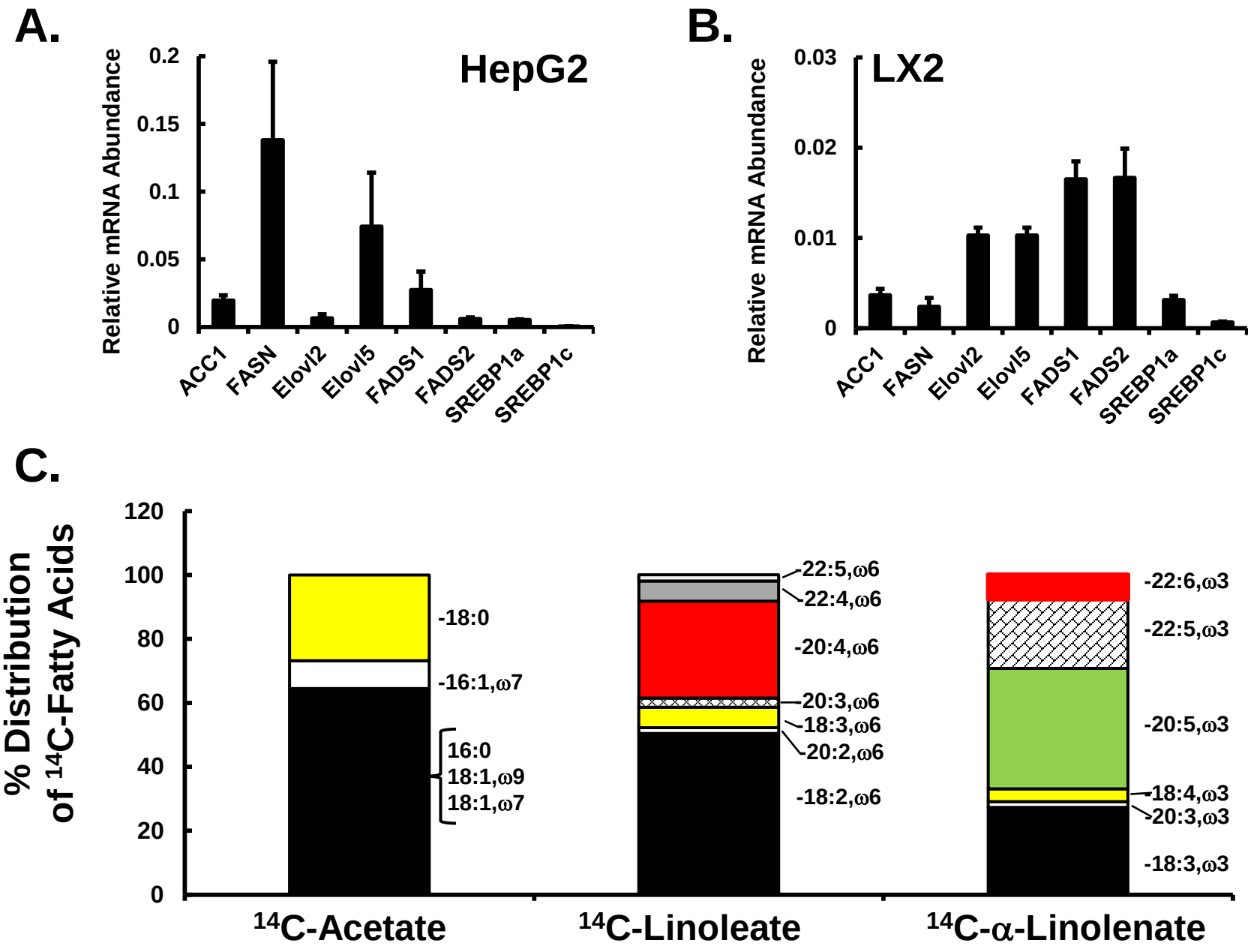

A. Chemokines & Cytokines

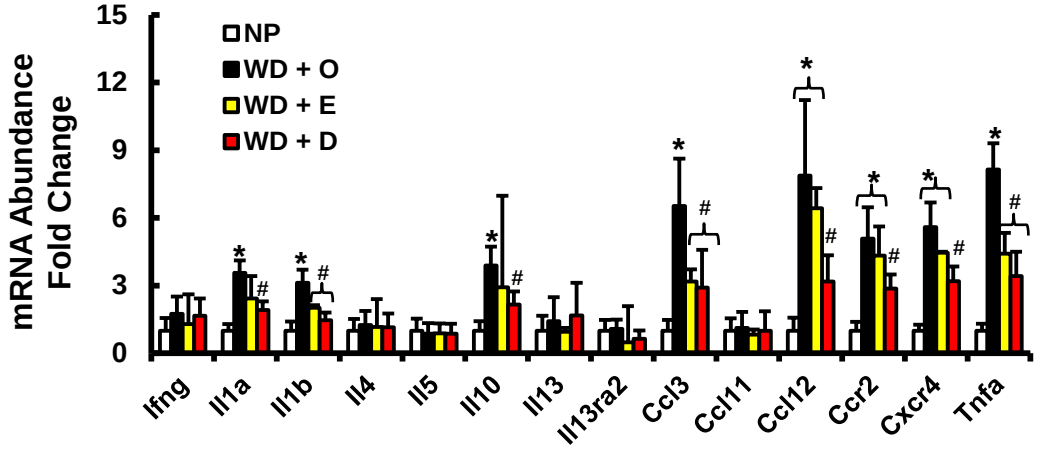

B. Growth Factors

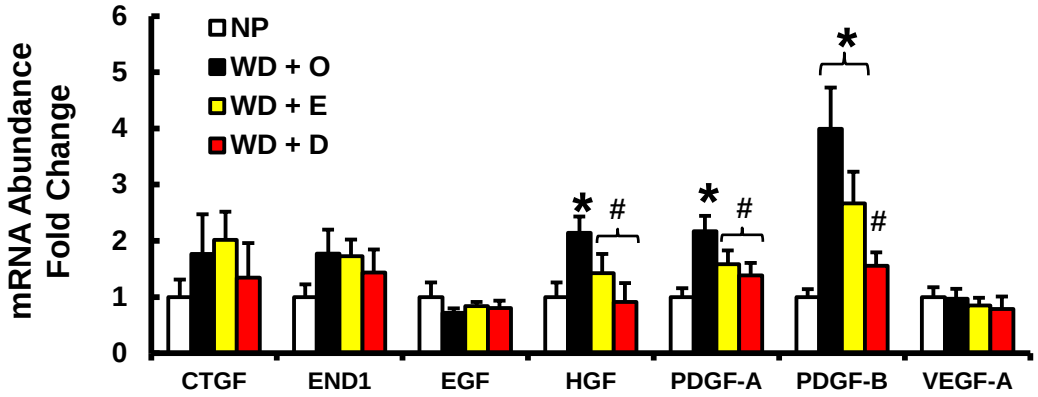

C. Transcription Factors

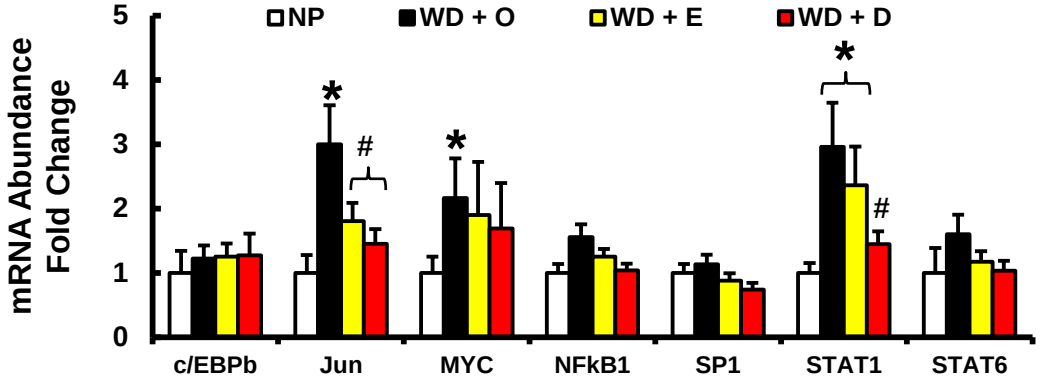

Supplement: Fig. 3S